Available online at www.sciencedirect.com

ScienceDirect

Procedia Engineering 10 (2011) 2719–2724

Engineering Procedia

ICM11

Fracture mechanics of porous ceramics using discrete element simulations

David Jauffrès[a], Xiaoxing Liu[a], Christophe L. Martin[a]*

[a]*Grenoble-INP, SIMAP laboratory, CNRS, UJF,DU, BP 46*
38402 Saint Martin d'Heres cedex, France

Abstract

The fracture behavior of highly porous ceramics is simulated using the discrete element method. A representative volume element made of spherical particles models the powder used to obtain a partially sintered ceramic material. Three-dimensional porous microstructures made of several tens of thousands of particles are then generated. Elastic force-displacement laws model the bonds formed between particles during sintering. A realistic fracture criterion, based on the local stress intensity factor associated with the bond between two particles, is also introduced. Based on these simulations, we compute the effective strength of these microstructures in tension as a function of the residual porosity. Furthermore, the introduction of a pre-crack in a sample subjected to a remote tensile stress allows the critical stress intensity factor to be calculated. Porous electrodes for electrochemical applications represent an important application field for these ceramics. Those discrete element simulations should be an effective tool for optimizing their microstructure at the submicronic length scale.

Selection and peer-review under responsibility of ICM11

Keywords: Discrete Element Method; porous ceramic; strength; toughness

1. Introduction

Porous ceramics obtained by partial sintering of powders are used for a wide range of applications including filtering, thermal insulation or electrodes for SOFC/SOEC (Solid Oxide Fuel Cells / Solid Oxide Electrolyser Cells).

The microstructures of these materials are often designed to enhance transport properties by increasing the pore volume fraction (typically from 20 to 50 %) and the surface area. However increasing the porosity drastically reduces their strength leading to failure issues. Also, in the case of electrochemical cells, localized cracking may not always lead to the full loss of the cell but can certainly decrease its electrochemical performances by breaking up the ionic and electronic conduction paths. It is thus critical to gain a better understanding of the fracture behavior of those porous ceramics in order to relate relevant microstructural parameters to the strength and the toughness of the material. In that respect, it is worth recalling that because those porous ceramics are made via powder sintering, their final microstructure retains a particulate architecture where initial particles are still observable.

* Corresponding author. Tel.: +0-000-000-0000 ; fax: +0-000-000-0000 .
E-mail address: christophe.martin@simap.grenoble-inp.fr

Selection and peer-review under responsibility of ICM11 doi:10.1016/j.proeng.2011.04.453

Much work has been carried out to model the influence of the porosity on the elastic modulus of ceramic materials [1-3], including Discrete Element Method (DEM) approaches [4; 5], but the fracture behavior of porous ceramics has been only rarely addressed [6].

DEM is a well fitted modeling tool to represent the complex microstructure of partially sintered porous ceramics. This is because in DEM, each particle is modeled as a distinct entity with specific mechanical interactions with its neighbors. Realistic microstructures can thus be generated by "numerical sintering" and then strained to characterize their mechanical behavior.

The aim of this study is to demonstrate the capability of DEM to obtain quantitative data on strength and toughness of partially sintered ceramics which should be of great interest for the microstructure optimization of this class of materials. In a first part, the strength is determined via the introduction of a bond fracture criterion in the model, and compared to experimental data on porous alumina. In a second part, it is shown that a fracture mechanic approach can be advantageously used to avoid the use of an adjustable parameter in the bond fracture criterion. The toughness of a given porous microstructure is obtained by applying Linear Elastic Fracture Mechanics (LEFM) to the simulation results of a sample containing a pre-crack and strained up to failure.

2. Model description

Only a brief description of the DEM principles and of the contact model is provided here. More details may be found in previous publications [5; 7; 8]. The DEM is based on the representation of material particles by discrete spheres that interact mechanically with each other through their contacts. The first stage of the simulation consists in generating a sintered porous sample by densifying a set of particles [8]. Then, the solid bonds that have formed between particles during sintering are modeled by elastic interactions, and the mechanical properties of the sample can be evaluated. Elastic interactions are defined by the normal N_b and tangential T_b contact forces between bonded particles following Jefferson's model [4]:

$$N_b = \frac{E}{1-\nu^2} f_N(\bar{\psi}) a_b u_N, \qquad T_b = -\frac{2E}{(2-\nu)(1+\nu)} f_T(\bar{\psi}) a_b u_T \tag{1}$$

where a_b is the contact radius, E and ν are the Young's modulus and Poisson ratio of the particles, f_N and f_T are functions of the particle radii, of the contact size and of a single geometric factor $\bar{\psi}$ [5]. u_N and u_T are the normal and tangential displacements. Similar equations relate the resisting moment in the normal and tangential directions to the accumulated relative rotations [4; 5].

Bond fracture is dictated by a critical strength σ_c that is compared to the normal and tangential stresses acting on the bond $\sigma_{bN} = N_b / \pi a_b^2$ and $\sigma_{bT} = T_b / \pi a_b^2$. σ_c is obtained by a stress intensity factor analysis assuming a stress singularity at the edge of the contact [9; 10]:

$$\sigma_c = \alpha \sqrt{\frac{E}{1-\nu^2}\frac{\Gamma}{\pi a_b}} \tag{2}$$

where Γ is the bond toughness that we approximate to the surface energy contribution ($2\gamma_s$). α is an adjustable geometric factor which value is known however for the simplified case of two spheres and a single contact (α=2) [9; 10]. To avoid unrealistic strength for very small bounds ($\sigma_c \rightarrow \infty$ when $a_b \rightarrow$ to zero), σ_c is limited to E/30.

Table 1. Alumina material parameters used for DEM simulation

Young's Modulus (E)	Poisson's ratio (ν)	Surface energy (γ_s)	Particle diameter
400 GPa	0.25	1 J/m^2	1 μm

After having their bonds broken, two neighboring spheres continue interacting elastically in compression and via the adhesive DMT model in tension [11]. The tangential resisting moment is kept, while the normal resisting moment is replaced by friction with a Hertz-Mindlin type tangential force in the sticking mode and a Coulomb

friction limit for sliding (friction coefficient = 0.5 used here). The DEM simulations performed in this study make use of the material parameters relevant for alumina reported in Table 1.

3. Strength

3.1. Sample generation

A gas of approximately 10,000 particles was first packed to a green density of 0.6 and then sintered to densities varying from 0.62 to 0.82. The samples generated are rectangular with a square base and a width to height ratio of 0.5. For a given density, five samples were generated from different initial particle seeding.

3.2. Results

The sintered samples are strained in the height direction via two planes while the lateral surfaces are kept with free boundary conditions and the fracture stress is recorded. As observed in Fig. 1, the stress vs strain curve is linear up to the fracture that initiates on a free surface and then propagates through the sample in a catastrophic manner. The geometric factor $\overline{\psi}$, which should be material independent, is fitted to obtain the macroscopic elastic properties of porous alumina [5].

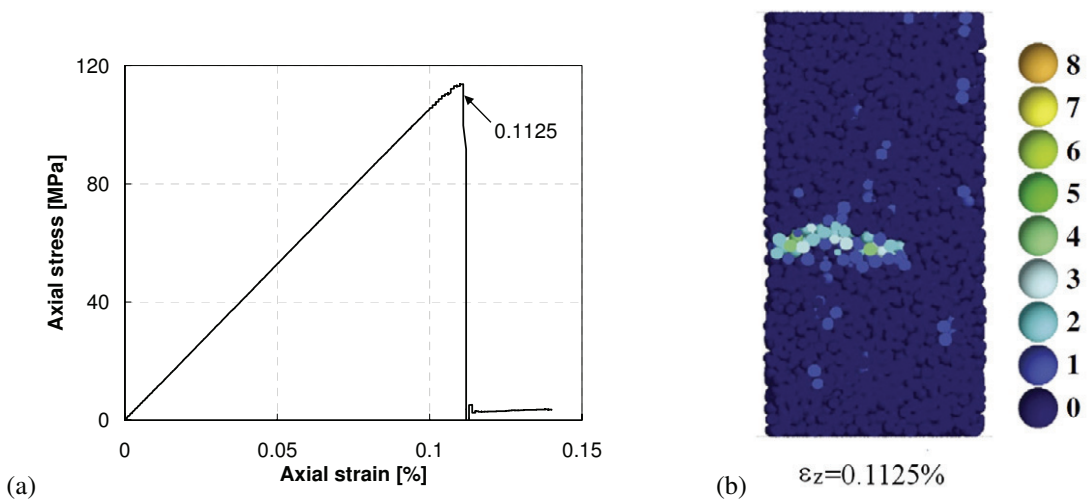

Fig. 1. Tensile test (a) Stress-strain curve (b) Crack propagation at ε_z=0.1125%. The color scale indicates the number of broken bonds for each particle

Fig. 2 shows the results obtained as a function of relative density for two values of α. A value α=1 leads to a reasonable agreement with experimental data. DEM estimation of fracture stress obtained with α=1 proves to be useful to study the effects of the microstructure on the strength of several porous ceramics [5; 12]. In that case, the porous microstructure is fairly homogeneous with no defect larger than the small pores left in between partially sintered particles.

However, fracture of brittle ceramics is known to initiate at process-induced defects [13]. The size of typical defects observed in ceramics and in particular in partially sintered alumina is around 20 μm to 50 μm [13; 14], i.e. in the order of magnitude of the DEM samples considered here. Consequently, no defects were included in our samples since it would require much larger numerical samples and prohibitive CPU time. Thus, it is not surprising that the fracture stresses obtained in our numerical defect-free samples and α=2 (which is believed to be a good approximation of the actual α value) overestimate the experimental values (Fig. 2).

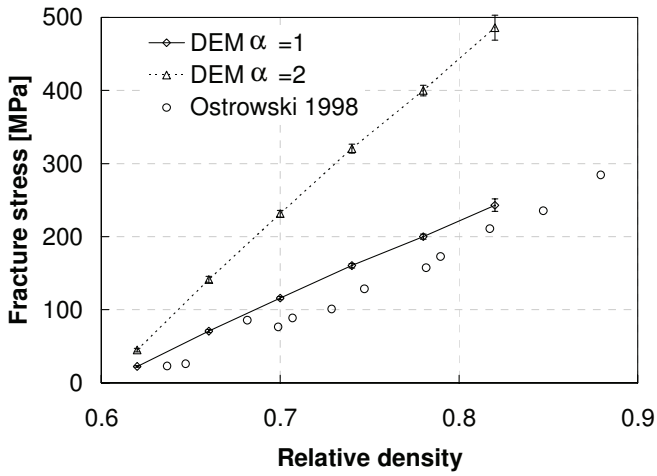

Fig. 2. Tensile fracture stress as a function of relative density for α=2 and α=1. Comparison with Ostrowski experimental data [14]. Error bars are calculated from five DEM simulations

4. Toughness

4.1. Linear Elastic Fracture Mechanics (LEFM)

To account for the influence of defects on the fracture strength σ_f of materials, the LEFM approach based on the relationship between the mode-I toughness KI_c (intrinsic property) and the critical flaw size can be used [15]:

$$\sigma_f = \frac{KI_c}{Y\sqrt{\pi a_c}} \tag{3}$$

Y is a geometric factor and a_c is the critical crack size. It is convenient to consider an idealized penny-shaped crack (Y=2/π) which defines the equivalent Griffith crack size of a critical defect of unknown shape. Experimental measurements of toughness are generally performed on pre-cracked notched samples with a known geometric factor. The same approach, using a sample with broken contacts simulating a pre-crack, is applied in DEM to compute the toughness using Eq. 3.

4.2. Sample generation

Samples with a similar microstructure to the one described in section 3 have been generated. They differ from the section 3 samples by their thickness and boundary conditions: instead of having a square base and free surfaces in x and y directions, the samples are thin plates (~ 5 particles thick) with periodic boundary conditions both in x and y. While free surface were needed to initiate fracture in strength testing, they are now useless as a pre-crack is introduced. It has been determined that the pre-crack should be at least 40 particles long to apply LEFM, thus leading to much larger samples (100,000 particles). Fig. 3a shows the 40-particles-long crack introduced and Fig. 3b the stress concentration around the crack tips. The geometry factor for a periodic array (width 2W) of collinear cracks (width 2a) is [15]:

$$Y = \left[\frac{2W}{\pi a}\tan\left(\frac{\pi a}{2W}\right)\right]^{0.5} \tag{4}$$

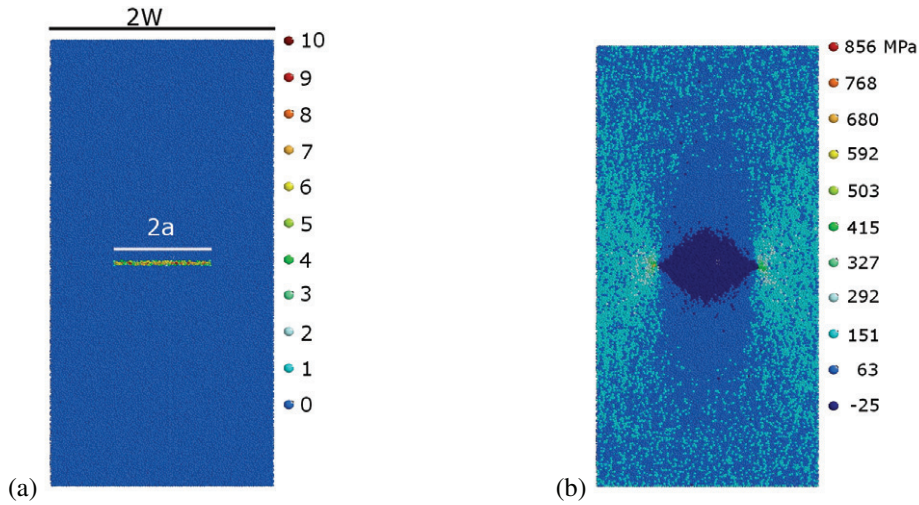

Fig. 3. (a) Toughness sample geometry showing the contacts broken to create the pre-crack (the color scale indicates the number of broken bonds for each particle). (b) Stress field in a pre-cracked sample before failure.

4.3. Results and discussion

The KI_c values deduced from the DEM simulations are plotted in Fig. 4a and compared to Ostrowski et al. experimental data [14]. Simulation data compare well the so-called crack tip toughness (K_0) of porous alumina similar in microstructure to our discrete model (one-micron particles free sintered with a green density of 0.61). Ostrowski et al. deduced K_0 for the whole density range from:

- an actual K_0 value obtained on a high density sample via the measurement of the Crack Opening Displacement,
- a proportional relationship between K_0 and E.

These authors claim K_0 to be more appropriate than KI_c conventionally measured on pre-cracked beam because of R-curve behavior even in porous alumina. This R-curve behavior is not accounted for in the model as perfectly brittle contacts are considered, which confirms that K_0 is the right parameter for comparison.

α has been set to 2, i.e. the value calculated from the stress intensity factor analysis conducted on two contacting particles [9; 10]. It is interesting to note that conversely to section 3, a good agreement is obtained with α=2 (Fig. 2 and Fig. 4a). The strength of a porous ceramic is linked to its critical defect which can hardly be accounted for in a DEM model and forced us to adjust α in section 3. The DEM fracture toughness approach eludes this necessity together with the question of the critical defect shape and size. This approach is more relevant for investigating the actual performance of the microstructure to resist crack propagation. It is thus believed to be a more practical parameter than fracture strength for microstructure optimization of porous ceramics via discrete simulations.

In addition, one can assume (or determine from micrographs if possible) a defect size and shape to obtain the fracture strength from KI_c. Here, for example, an acceptable agreement with experimental strength is obtained from DEM toughness assuming an idealized penny-shaped crack with a 30µm radius (Fig. 4b). This defect size is in reasonably good agreement with the order of magnitude of flaws observed by Ostrowski et al. [14].

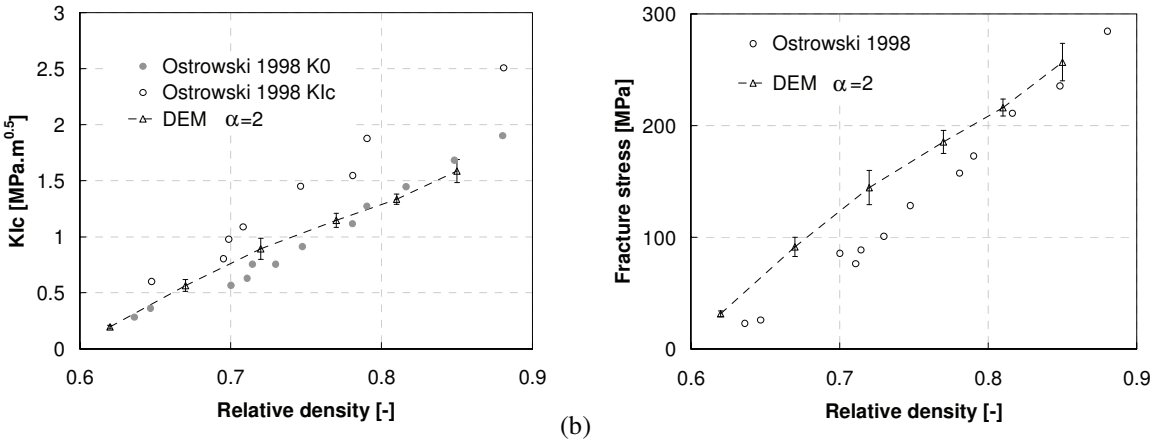

Fig. 4. (a) Fracture toughness (b) Toughness-deduced fracture stress assuming an equivalent Griffith crack size of 30μm. Error bars are calculated from five DEM simulations.

5. Conclusion

DEM simulations were conducted on microstructures typical of partially sintered ceramics in order to investigate their fracture behavior. A first approach consists in recording the fracture stress of homogeneous samples that do not contain defects larger than the microstructure characteristic length scale. However, large defects are believed to control the strength of partially sintered ceramic materials. To tackle the difficulty of incorporating realistic defects within DEM samples it is possible to study the fracture toughness KI_c by introducing a pre-crack and applying LEFM. KI_c values obtained by DEM over a large density range agree reasonably well with experimental data, thus validating the approach used here.

Acknowledgements

The Agence Nationale pour la Recherche (ANR), PAN'H and Blanc programs, is greatly acknowledged for financial support (MOISE and OPTIMA_SOFC projects)

References

[1] A .P. Roberts , E .J. Garboczi, Journal of the American Ceramic Society 83 (2000) 3041.
[2] W. Pabst, E. Gregorová , G. Tichá, Journal of the European Ceramic Society 26 (2006) 1085.
[3] R. Rice, Journal of Materials Science 40 (2005-02-28) 983.
[4] G. Jefferson, G .K. Haritos , R .M. McMeeking, Journal of the Mechanics and Physics of Solids 50 (2002)2539.
[5] X. Liu, C .L. Martin, G. Delette , D. Bouvard, Journal of the Mechanics and Physics of Solids 58 (2010) 829.
[6] D. Leguillon , R. Piat, Engineering Fracture Mechanics 75 (2008) 1840.
[7] C .L. Martin, D. Bouvard , S. Shima, Journal of the Mechanics and Physics of Solids 51 (2003) 667.
[8] X. Liu, C .L. Martin, G. Delette, J. Laurencin, D. Bouvard , T. Delahaye, Journal of Power Sources 196 (2011) 2046.
[9] H. Fujita, G. Jefferson, R .M. McMeeking , F .W. Zok, Journal of the American Ceramic Society 87 (2004) 261.
[10] L .B. Freund , E. Chason, J Appl Phys 89 (2001) 4866.
[11] B .V. Derjaguin, V .M. Muller , Y .P. Toporov, Journal of Colloid and Interface Science 53 (1975) 314.
[12] X. Liu, C .L. Martin, G. Delette, J. Laurencin, S. Di Iorio , D. Bouvard, submitted to acta materialia (2011) .
[13] R. Danzer, T. Lube, P. Supancic , R. Damani, Advanced Engineering Materials 10 (2008) 275.
[14] T. Ostrowski, A. Ziegler, R .K. Bordia , J. Rödel, Journal of the American Ceramic Society 81 (1998) 1852.
[15] T .L. Anderson, Fracture Mechanics. Fundamentals and Applications. 3rd Edition., CRC Press, 2005.